



### **Science Arts & Métiers (SAM)**

is an open access repository that collects the work of Arts et Métiers Institute of Technology researchers and makes it freely available over the web where possible.

This is an author-deposited version published in: <https://sam.ensam.eu>  
Handle ID: <http://hdl.handle.net/10985/19856>

#### **To cite this version :**

Kevin MARCHAIS, Jeremie GIRARDOT, Charlotte METTON, Ivan IORDANOFF - A 3D DEM simulation to study the influence of material and process parameters on spreading of metallic powder in additive manufacturing - Computational Particle Mechanics p.1 - 2021

Any correspondence concerning this service should be sent to the repository

Administrator : [scienceouverte@ensam.eu](mailto:scienceouverte@ensam.eu)



# A 3D DEM simulation to study the influence of material and process parameters on spreading of metallic powder in additive manufacturing

K. Marchais<sup>1,2</sup>  · J. Girardot<sup>1</sup> · C. Metton<sup>2</sup> · I. Iordanoff<sup>1</sup>

## Abstract

The aim of this work is to understand the granular behavior of metal powder during the spreading phase of the LBM process in order to study the effect of powder properties and process parameters on the quality of the layer deposited before laser fusion. This is a numerical work performed with simulations based on the discrete element method where each powder grain is simulated. The numerical model takes into account different interactions such as repulsion, dissipation, friction and adhesion that occur when there is contact between two bodies. The powder grains are assumed to be perfectly spherical. The surface roughness of the plate and spreader is taken into account in the simulations as it has a significant impact on the powder bed spreading. The effect of material parameters such as friction and adhesion is studied. The influence of the spreading speed is also studied. The results show that different friction values give the same results on the final properties of the powder bed while adhesion plays a significant role. Finally, lower spreading speed result in a better powder bed.

**Keywords** Laser beam melting · Additive manufacturing simulation · Discrete element method · Granular behavior · Powder spreading

## 1 Introduction

In metallic powder-bed-based additive manufacturing processes, for each layer of matter, 2 main phases occur. First, there is the powder spreading to form a powder bed, then there is the laser scanning to melt selected zones that correspond to the sections of the fabricated part. In order to produce pieces of better quality, faster and at the lowest cost, it is important to study the influence of the different process parameters to determine the best configurations of parameters on the deposited powder layer. Studies about powder deposition in additive manufacturing processes started recently, this work takes part in this domain of study. According to the grains disposition in the powder bed, laser-matter interactions can

be impacted and can affect the quality of the final fabricated part. Indeed, if the powder bed is not dense enough or heterogeneous, some issues can happen such as porosity, lack of matter, balling effect, etc. Zielinski et al. [1] studied the influence of the powder grains layout on laser melting with comparison between spreaded powder bed and body-centered cubic (BCC) structured powder bed and showed that BCC powder bed produces a homogeneous melting whereas spreaded powder bed shows irregular melt pool. Then it is important to understand which parameters influence the final powder bed quality. Production time is impacted by the time of the powder spreading phase because a large number of layers is needed to produce a piece (e.g., 5000 layers of 60 µm needed for a height of 30 cm). One can want to increase spreader speed or increase the thickness of deposited layers to speed up the spreading phase but how does it affect final powder bed quality? Some machines use a blade as coating system while others use a roller or a brush. Some spreaders are rigid (metals), others are flexible (silicon). Haeri [2] studied the optimization of the spreader geometry to enhance powder bed quality and obtain better powder bed than with a roller or a classic blade.

---

✉ K. Marchais  
kevin.marchais@ensam.eu

<sup>1</sup> Arts et Metiers Institute of Technology, Univ. of Bordeaux, CNRS, Bordeaux INP, INRAE, I2M Bordeaux, F-33400 Talence, France

<sup>2</sup> Safran Additive Manufacturing, a technology platform of Safran Tech, Rue des Jeunes Bois, Châteaufort, 78114 Magny-Les-Hameaux, France

Fouda et al. [3] studied the effect of spreader speed and gap thickness on packing fraction and particles velocities with monodisperse (every particle has the same size) powder samples. They showed that the packing fraction could be enhanced by varying spreader speed and gap thickness. Chen et al studied the effect of spreading powder with counter-rolling roller as spreader and showed that increasing spreading speed decreases powder bed packing density and surface quality [4].

Depending on the material, the grain size or powder distribution, the final powder bed quality is different. Indeed, the material parameters such as adhesion combined with smallest particles highly deteriorates powder bed quality due to the formation of clusters and cavities as shown by Chen et al. [5,6] and Meier et al. [7] on TiAl6V4 powders. In this case, adhesion forces become very important compared to the grains weight.

Then the study of the adhesion parameter is fundamental. One of the cause of adhesion in powder is humidity. Higher is the humidity, higher is the adhesion. In LBM process, humidity level is extremely low so there are only Van der Waals' forces that play the role of adhesive force. However, it could be interesting to understand if less strict environment and powder storage conditions could lead to good results in powder bed quality in order to reduce the production costs. Then it is important to understand how does adhesion affect powder spreading in order to know in what conditions should be stored the powder and if powder spreading should be done under controlled atmosphere or not for example. Powders material parameters are complicated to indentify for these models and the best solution seems to be the measurement of the repose angle of powder samples as Meier et al. did [8].

Several studies have been realized about Selective Laser Sintering (SLS) process which is very close to Laser Beam Melting (LBM) as a laser is used to transform a spreaded powder bed. The difference is about the material used in the process as LBM uses metallic powders whereas SLS uses polymeric powders. For example, Parteli and Pöschel [9] studied the spreading of PA12 powders (polymer) and have taken into account the non-sphericity of the particles by simulating complex shape with multisphere method, and Haeri et al. [10] studied the spreading of rod-shaped polymeric particles with rollers as spreaders.

In metal powder-based processes, the particles are highly spherical thanks to the gas/water atomization process [11]; however, Nan and Ghadiri [12] applied the multisphere method to 316L samples which presents less spherical grains than inconel or titanium-based powders.

The grains size is of the order of magnitude of the surface roughness properties of the plate or substrate. Then the surface roughness has to be taken into account. Nan and Ghadiri [12] chose to simulate surface roughness with cylinders arranged side by side.

So until now, only a few studies focus on the powder bed spreading simulation. The cited studies use the discrete element method to simulate powder behavior. This study, also based on discrete element method, aims to understand the behavior of polydisperse metallic powders with highly spherical particles and show the influence of surface roughness and spreader speed on powder bed properties. The influence of material parameters such as friction and adhesion is also studied in order to have a better knowledge on how precisely these parameters must be determined.

First, the numerical model developed to realize this study will be presented. Then, the results of preliminary studies including surface roughness influence will be presented. Finally, the parametric study and the obtained results will be discussed.

## 2 Numerical model

### 2.1 Numerical method

The Discrete Element Method (DEM), initially presented by Cundall [13], is the chosen method to realize the simulations of this study as it is particularly adapted to granular media simulations. Each powder grain is represented by a discrete element, and the fundamental principle of dynamics is applied to each of them in order to get their acceleration. Then, by integration (Verlet velocity scheme), the velocity and the displacement of each element are computed. The forces that are considered in the simulations are gravity and interactions forces between the bodies. Simulations are computed in 3D with the open-source platform GranOO developed in C++ [14] and based on the Discrete Element Method. This method considers small interpenetrations between the particles to detect a collision between two particles. Unlike polymeric powder [9], metal grain powders are very spherical but can present small satellites at their surface. In this study, the particles are supposed perfectly spherical and satellites are not taken into account.

### 2.2 Choice of interaction forces

When a contact occurs between 2 bodies, a repulsion force is generated. There is also normal energy dissipation that is taken into account with a damping coefficient. There can also be a force that tends to maintain contact between bodies if they are adhesive. Finally, a friction force is applied if the relative velocity between the two bodies is not collinear to the contact direction. These 4 forces are detailed below:

### 2.2.1 Repulsive force

Modeling of the repulsion between two grains with a contact stiffness (Eq. (1)). This is a normal force.

$$\vec{F}_r = k\delta \vec{n} \quad (1)$$

where  $k$  is the contact stiffness (N/m),  $\delta = R_1 + R_2 - d_{12}$  is the interpenetration between the grains, with  $R_1$  and  $R_2$  the radii of the particles and  $d_{12}$  the distance between their centres,  $\delta < 0$  when there is a contact.

Other models are used to model the repulsion between the grains such as the Hertz contact model [15]. It considers the slight deformation of two spheres that are in contact and take into account Young modulus and Poisson coefficient of materials (Eq. (2)).

$$\vec{F}_H = \frac{4}{3} E^* \sqrt{R^*} \delta^{\frac{3}{2}} \vec{n} \quad (2)$$

However, the high value of Young modulus makes the contact stiffness very high. The time-step is depending on the contact stiffness and the grain mass according to the condition (3) (spring-dashpot model).

$$\Delta t < 0.2 \sqrt{\frac{M_{\min}}{k}} \quad (3)$$

The additive manufacturing powder is constituted by grains whose diameter is the size of a few microns. For particles of this size, the mass is very low. It results with a very low time-step. The high computation cost of the Discrete Element Method do not allow to use Hertz model in this case because of high values of Young modulus. To obtain reasonable time computation, a higher time-step is needed. Studies using Hertz model reduce Young modulus as it doesn't affect the powder behavior as shown by Chen et al. [16]. Meier et al. [8] also showed that modifying the stiffness value doesn't affect the results of powder pile simulation. The contact stiffness is then modified because it does not impact the global granular behavior with the tested values. Nevertheless, some conditions must be respected : the interpenetration must be limited to avoid numerical issues. Then the contact stiffness must be high enough to face adhesion force and particles weight.

### 2.2.2 Energy dissipation

When there is a contact, a part of the energy is dissipated. The chosen model to represent it is described by Eq. (4) :

$$\vec{F}_d = 2\alpha \sqrt{kM} V_{rel} \vec{n} \quad (4)$$

where  $\alpha$  is the dissipation coefficient,  $M$  the reduced mass of the two grains in contact,  $V_{rel}$  the relative velocity of the bodies in contact. This model allows to link easily the dissipation coefficient to the restitution coefficient  $\epsilon$  often used in granular problems with the relation  $\alpha = \frac{1}{\sqrt{1 + \left(\frac{\pi}{\ln(\epsilon)}\right)^2}}$

### 2.2.3 Adhesion

When 2 bodies are in contact, there is a surface energy that creates an attractive force between them. The chosen model to represent this phenomenon is described by Eq. (5). This one is very close to the JKR model [17] and DMT model [18] that accounts for Van der Waals forces and is also close to models that allows to represent adhesion with liquid bridges when the humidity level is high enough in the powder [20]. JKR, DMT and liquid bridges models have the same shape of equations where a coefficient is multiplied by  $R^*$ . This coefficient is constant with JKR and DMT models. So it has been chosen to take  $\gamma$  as the whole constant and to determine its value.

$$\vec{F}_a = \gamma R^* \vec{n} \quad (\text{when } \delta < 0) \quad (5)$$

with  $\gamma$  the surface energy ( $J/m^2$ ) and  $R^* = \frac{R_1 R_2}{R_1 + R_2}$  (m) the equivalent radius corresponding to the two grains.

### 2.2.4 Friction

When 2 bodies are in contact and in movement, a force is opposing to the tangential relative displacement for each body. This is the friction that is simulated by Coulomb law (Eq. (6)). This model could also allow to represent the satellites fixed around the powder grains [21], increasing artificially the macroscopic friction between 2 grains.

$$\vec{F}_t = -\mu \left( V_{rel}^T \right) \|\vec{F}_r\| \vec{t} \quad (6)$$

The friction coefficient  $\mu$  depends on the relative velocity between the 2 bodies. If the tangential component of the relative velocity is positive, then the friction coefficient is equal to  $+\mu$ , else if it is negative then it is equal to  $-\mu$  (Fig. 1). When the relative velocity tends to zero, the function must be regularized.  $\vec{t}$  is the tangential vector to the contact.

The principle of this method is represented in Figs. 2 and 3 by the contact between 2 particles with given velocities. The forces generated by the contact are represented by the normal and tangential components of the total resulting force. Here, there is a regularization of the repulsive force by accepting an interpenetration  $\delta$  and of the friction force by the calculation of the  $\mu$  factor. This is a notable characteristic of this numerical method. On the opposite, the Non-Smooth Contact Dynamics [22] manages non regularized forces.

**Fig. 1** Regularization of the Coulomb's law

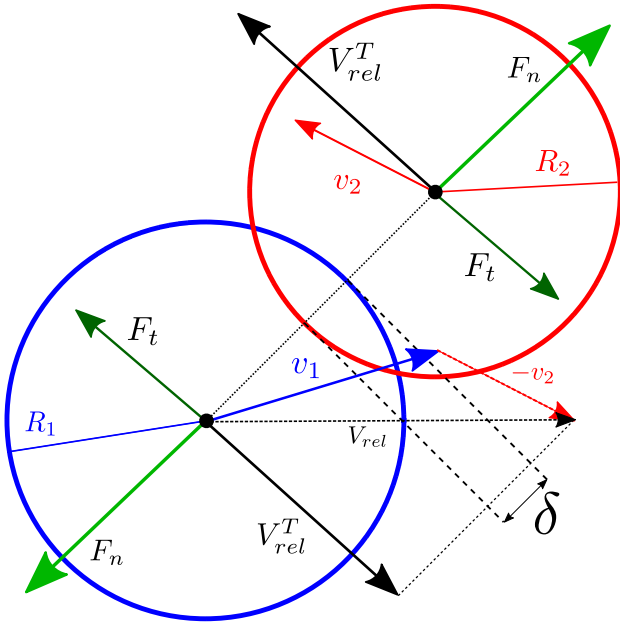
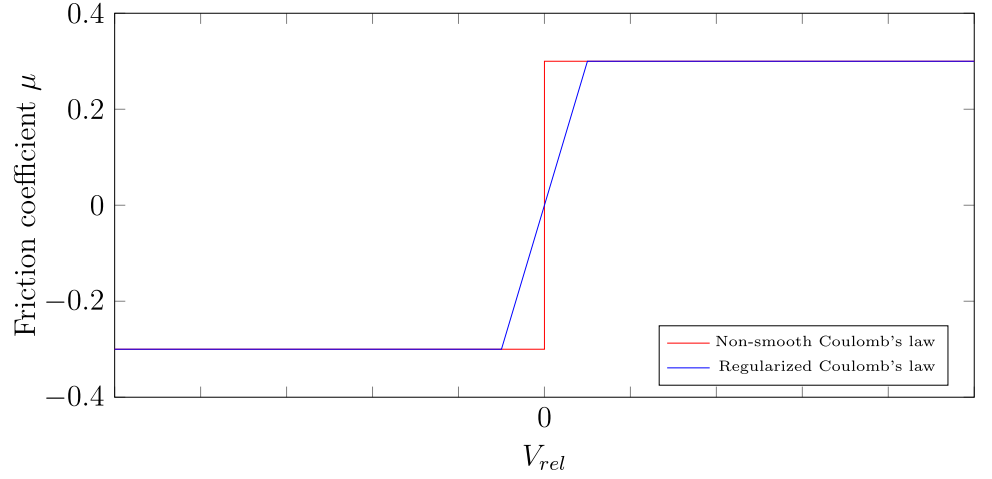


**Fig. 2** DEM scheme

**Integration of acceleration** In order to compute particles motion, acceleration can be computed with the sum of the forces acting on the particle (interaction forces and weight) and its mass. Then velocity and position can be computed from acceleration using Verlet velocity integration scheme (Eq. (7)).

$$\begin{cases} a_{n+1} = \sum \vec{F} / M \\ v_{n+1} = \frac{1}{2} \Delta t (a_{n+1} + a_n) \\ p_{n+1} = v_{n+1} \Delta t + a_{n+1} \Delta t^2 \end{cases} \quad (7)$$

with  $a$  the acceleration,  $v$  the velocity and  $p$  the position,  $M$  the mass of the particle and  $\sum \vec{F}$  the sum of the forces applied on the particle.

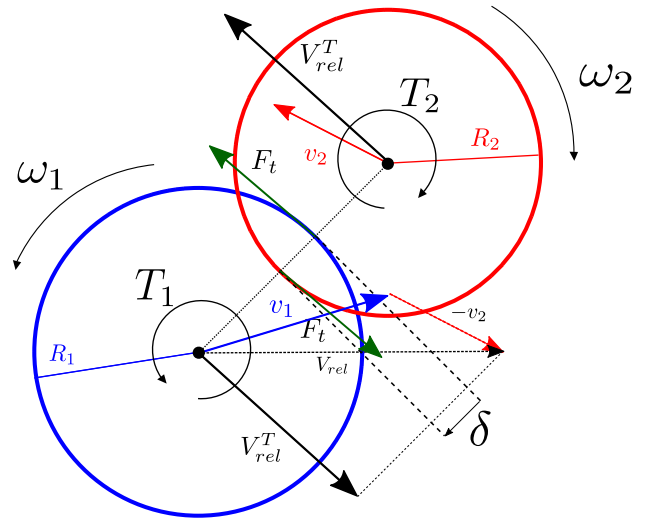


**Fig. 3** Angular motion

Angular acceleration and velocity are also computed to get the particles rotation with the use of quaternions which allows quick computations of rotations. Angular acceleration is given by Eq. (8) [23,24].

$$\alpha_{n+1} = \omega_n \cdot \bar{\theta}_n \cdot \omega_n + \frac{1}{2} \theta_n \left[ I^{-1} \left( \sum \vec{\tau} - 4(\bar{\theta}_n \cdot \omega_n) \wedge I.(\bar{\theta}_n \cdot \omega_n) \right) \right] \quad (8)$$

with  $\alpha$  the angular acceleration,  $\omega$  the angular velocity,  $\theta$  the rotation,  $I$  the moment of inertia of the particle and  $\sum \vec{\tau}$  the sum of the torques applied on the particle. Then angular velocity and rotation can be computed with Verlet velocity integration scheme (Eq. (9)).

$$\begin{cases} \omega_{n+1} = \frac{1}{2} \Delta t (\alpha_{n+1} + \alpha_n) \\ \theta_{n+1} = \omega_{n+1} \Delta t + \alpha_{n+1} \Delta t^2 \end{cases} \quad (9)$$

**Table 1** IN718 powder sample deciles

Sample	$D_{10}$ $\mu\text{m}$	$D_{50}$ $\mu\text{m}$	$D_{90}$ $\mu\text{m}$
Real	21	31	49
Numerical	20	31	43

### 2.3 Domain of study

To realize this study, all the simulations are computed with the same base geometry shown in Fig. 4. It contains a first plate where powder is put before the spreading (blue grains) and the fabrication plate on which powder is spread. The second plate is a little lower than the first in order to correspond to the wanted layer thickness. In this study, powder spreading is studied exclusively on a rigid and rough surface. There is no spreading on a previous non-melted powder layer. The spreader is a supposed infinitely rigid blade with a speed  $V$ .

In the fabrication zone, a layer is already existing (red) in order to simulate the surface roughness of the melted previous layer. The red layer contains discrete elements that cannot move. It allows to simulate plate/substrate surface roughness. A melted surface has a roughness of the order of magnitude of the grains size, so the irregular surface created by the discrete elements allows to approach the real roughness of the substrate. The plates width is 300  $\mu\text{m}$ , and periodic boundary conditions are applied in the transverse direction in order to simulate infinite width. The plates length is 4 mm. The studied domain is relatively small because the numerical method is very expensive in calculation time, so the number of discrete elements must be limited. Nevertheless, this length is long enough to observe the powder global behavior during the spreading. The material taken into account for this study is a metallic powder of IN718 which powder grains are very spherical. Simulations are computed with spherical grains with a size distribution that follows a normal law with a diameter of 30  $\mu\text{m}$  and a standard deviation of 10  $\mu\text{m}$  that is similar to measured IN718 powder samples. For example, Table 1 compares a measure of virgin IN718 powder sample deciles reported by Nguyen et al. [25] with numerical particle size distribution.

Each layer has approximately 10000 discrete elements. The parameters values used in the simulations are reported in Table 2. The contact stiffness is 0.1 N/m because it allows to have small enough interpenetrations between the grains and an acceptable calculation time (around 10h). The overlap between 2 particles must be very small in order to keep the simulation stable. The condition fixed here is the following  $\frac{\delta}{R} < 10^2$  with  $\delta$  the overlap and  $R$  the radius of the particle. The contact stiffness must be high enough to balance with weight or adhesion force. Restitution coefficient is set to 0.1 to stabilize the simulation. Meier et al. [8] showed that contact

**Table 2** Simulation parameters

Parameter		Value
$\rho$	Density ( $\text{kg/m}^3$ )	8000
$d$	Diameter of a particle ( $\mu\text{m}$ )	7–70
$L$	Plate length (mm)	4
$V$	Recoater speed (mm/s)	50–250
$k$	Contact stiffness (N/m)	0.1
$e$	Restitution coefficient	0.1
$\gamma$	Adhesion energy ( $\text{mJ/m}^2$ )	0–10
$\mu$	Friction coefficient	0–0.9

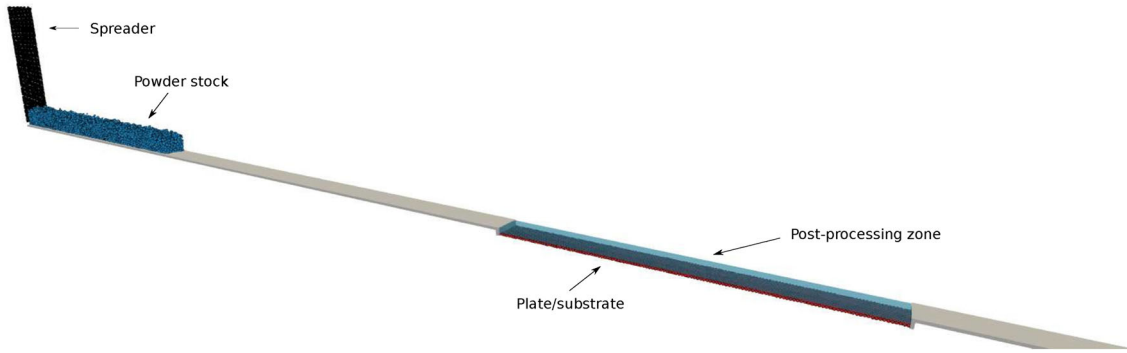
stiffness and restitution coefficient can be modified without affecting powder behavior. The other parameters are variable.

Figure 5 shows the powder behavior during the spreading. The spreader collects the powder on the first plate, and a pile is forming ahead of it as shown with experimental results by Chen et al. [6]. When the spreader reaches the fabrication zone, the powder spills under the spreader to form the new layer.

### 2.4 Powder bed properties

In order to compare the final powder bed for different parameters configurations, it is important to define properties that will permit to analyze its quality. The chosen measured properties are the packing fraction, the coordination number and the average grain size. Pieces produced by LBM process can present a high level of porosity if the powder bed is not dense enough. The packing fraction must then be as high as possible to minimize the porosity and allow the best melting efficiency. The study of the average grain size can be interesting according to the position in the powder bed to check segregation phenomenon that has already been observed on experimental testings. This phenomenon has already been observed in other domains such as mixers for example [26]. In spreading process, the powder flow could result in the fact that small particles would rather be at the beginning of the spreading zone whereas bigger particles would be at the end. Finally, the coordination number is the average number of contacts per grain. This parameter is strongly linked to powder bed thermal conductivity since there is better thermal conduction through solid matter than through gas. It is then important to get a high and homogeneous coordination number. A post processing zone is set and identified by the blue zone in Fig. 4 in the powder bed. This zone is subdivided (Fig. 6) to compute properties in each cell and compare it through the position in the powder bed. The packing fraction is computed by the ratio between the volume of each grain belonging to a cell and the volume of the cell.





**Fig. 4** Domain of study

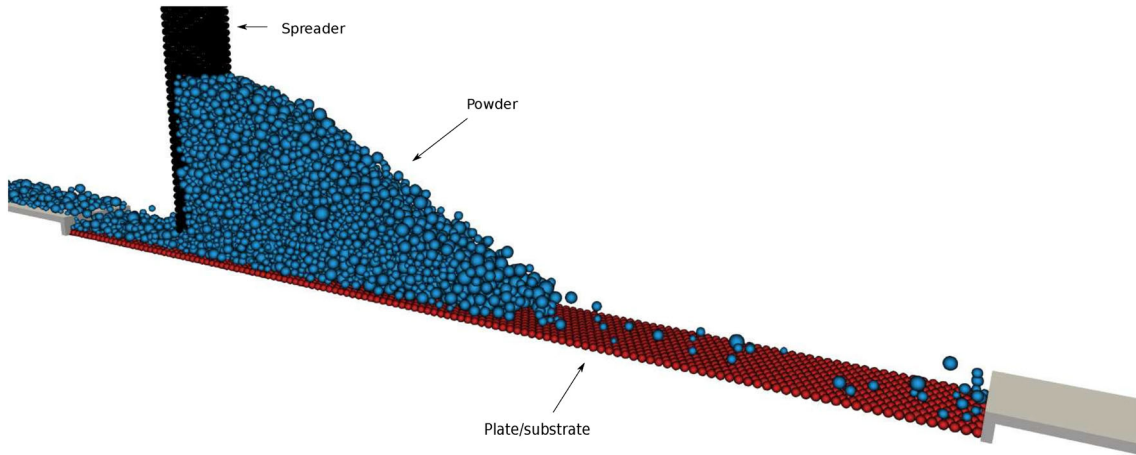


**Fig. 5** 3D simulation of powder spreading

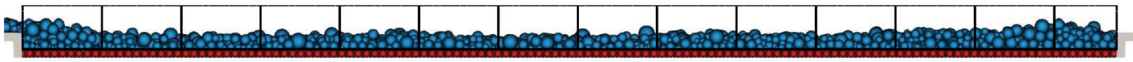


**Fig. 6** Subdivision of the post-processing zone

## 2.5 Surface roughness

It has been chosen to take into account plate (or substrate) surface roughness because this is supposed to be of significant impact on powder spreading and final powder bed properties. To simulate the surface roughness, Nan et al. [12] chose to use

clumped cylinders. In this study, the chosen method consists in disposing discrete elements regularly as shown in Fig. 7. First, it allows to control the roughness parameters by adjusting the discrete elements diameters. Then, contrary to Nan et al, the roughness is taken into account in every directions.

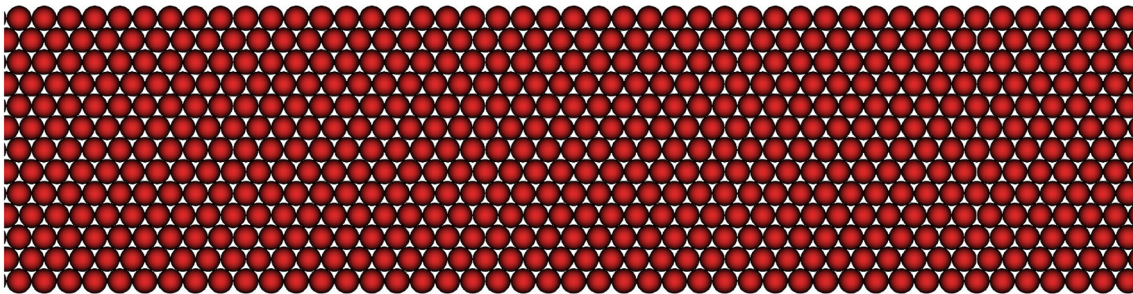


**Fig. 7** Rough plate (top view)

**Table 3** Roughness effect on global powder bed density

Roughness	Density (%)
Smooth	49.64
7 $\mu\text{m}$	46.79
30 $\mu\text{m}$	53.97
50 $\mu\text{m}$	63.09

However, these methods create a regular roughness whereas real part surface roughness is more random.

Simulations have been computed with different discrete elements diameters to highlight the surface roughness influence on powder flow and powder bed properties. Figure 8 shows the impact of surface roughness on powder spreading as the angle of the powder pile ahead of the spreader is increasing as the surface roughness increases. Table 3 lists powder bed density for each case, and it shows that the powder bed is more dense with a higher surface roughness. So surface roughness affects the powder flow and the final powder bed quality. For the following studies, the surface roughness is simulated with particles diameters of 30  $\mu\text{m}$ .

### 3 Results

The following studies are part of a parametric study where the goal is to observe the influence of a material or process parameter by varying it. For all the studies, all parameters are fixed except the parameter that is being investigated. The friction coefficient is set to  $\mu = 0.3$ . The adhesion energy is set to  $\gamma = 0 \text{ mJ/m}^2$  in order to not make appear adhesion effect when studying the effect of other parameters. The spreader speed is set to 100 mm/s. The chosen particle size distribution follows a normal law with an average diameter of 30  $\mu\text{m}$ , a standard deviation of 10  $\mu\text{m}$ , a minimal diameter of 7  $\mu\text{m}$  and a maximal diameter of 70  $\mu\text{m}$ . Especially for material parameters, the aim of these studies is to understand the influence of the parameter and determine how precisely it should be identified with further experiments.

#### 3.1 Friction coefficient effect

The influence of friction coefficient on powder bed spreading is necessary to understand to evaluate the precision needed in this coefficient characterization. Even if for a given material, the friction coefficient is a proper material parameter, this study permits to understand the powder behavior whose friction coefficient is more or less high. As Fig. 9 shows, the powder bed seems to have globally the same properties for the studied parameters values ( $\mu = 0$ ,  $\mu = 0.01$ ,  $\mu = 0.1$ ,  $\mu = 0.3$ ,  $\mu = 0.9$ , large range of metal friction coefficient) and no tendency is emerging. According to these results,

the friction coefficient has not a consequent impact on the spreading process so it will be assumed to be constant for the following.

Friction has no influence on granular behavior during powder spreading so it is not necessary to identify precisely its value. Then the effect of adhesion energy, the second material parameter, will be studied.

#### 3.2 Adhesion energy effect

As for the friction, the adhesion depends also on the powder sample material studied but also on the environment such as humidity level. It is necessary to understand the behavior difference between a non-adhesive powder and a more or less adhesive powder. Simulations have been computed with different adhesion energies ( $\gamma = 10 \text{ mJ/m}^2$ ,  $\gamma = 5 \text{ mJ/m}^2$ ,  $\gamma = 1 \text{ mJ/m}^2$ ,  $\gamma = 0.5 \text{ mJ/m}^2$ ,  $\gamma = 0.1 \text{ mJ/m}^2$ ,  $\gamma = 0 \text{ mJ/m}^2$ , the maximum adhesion value is chosen after numerical flow tests that showed that powder flow was very deteriorated with  $\gamma = 10 \text{ mJ/m}^2$ ). Figure 10 shows that adhesion has an important impact on the final powder bed. Density and coordination number evolve in opposite directions. For a very adhesive powder, there will be particles heaps where the density will be locally very high (high coordination number) but also cavities that deteriorate the average powder bed density as shown in Figs. 10 and 11.

On the contrary, the powder bed obtained with non-adhesive powder is rather dense but with a low coordination number compared to the other testings. The simulations realized with  $\gamma = 1 \text{ mJ/m}^2$  and  $\gamma = 0.5 \text{ mJ/m}^2$  provide a density similar to the ones provided with  $\gamma = 0 \text{ mJ/m}^2$  with a much higher coordination number.

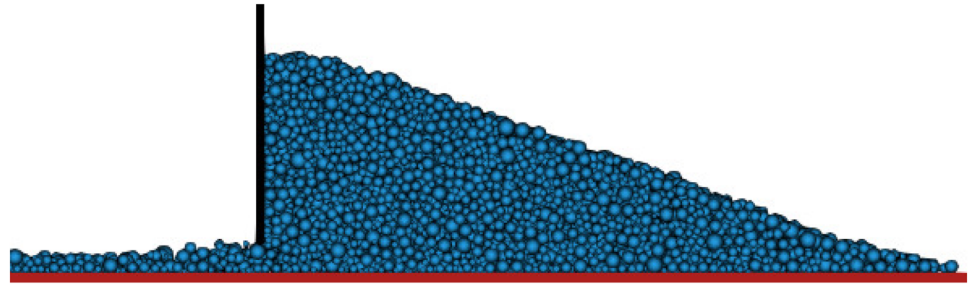
Unlike friction coefficient, adhesion energy has a significant effect on powder bed final properties. This parameter will have to be precisely identified in order to compute powder bed spreading simulations. The following studies treat on process parameter influence beginning with spreader speed influence on powder bed properties.

#### 3.3 Influence of the spreader speed

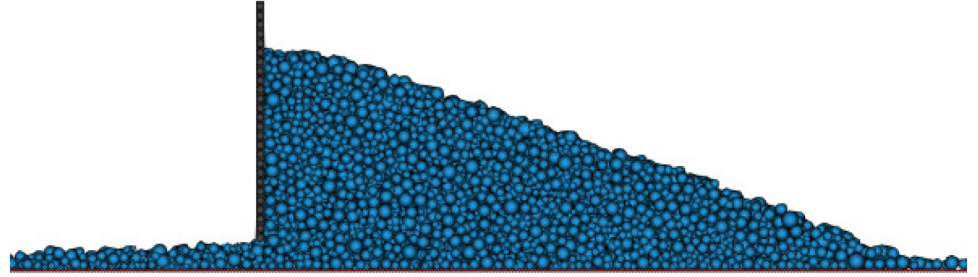
In order to observe the spreader speed influence on the powder bed final properties, several simulations have been computed with different speeds ((50, 75, 100, 125, 150, 175, 200, 225 and 250 mm/s). Figure 12 shows the evolution of the density, of the average grain size and of the coordination number according to position for the following velocities: 50, 100, 150, 200 and 250 mm/s. As expected, slower the spreading is, better the powder bed density is and higher the coordination number is. Indeed, the obtained density for a speed of 50 mm/s exceed 60% whereas for the higher speed (250 mm/s), the powder bed is less dense (40–50%). The values measured at the first and last positions are not the



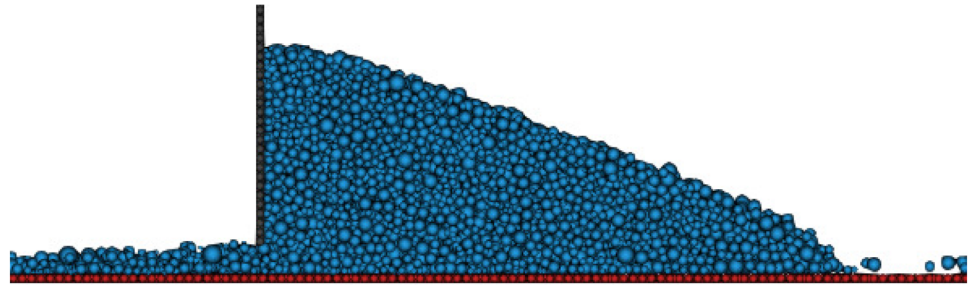
**Fig. 8** Surface roughness influence



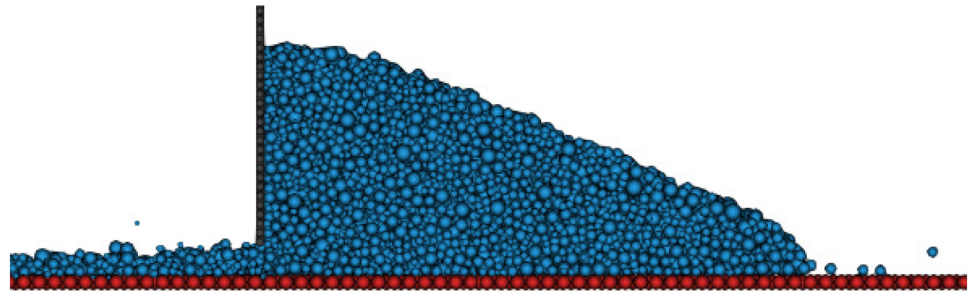
(a) Smooth plate



(b)  $\varnothing = 7 \mu m$



(c)  $\varnothing = 30 \mu m$



(d)  $\varnothing = 50 \mu m$

most representative data since it corresponds to the lack of matter caused by the grains inertia for the first case and by the fall of the grains beyond the plate for the second. Moreover, at high velocities, the powder bed is not homogeneous. The density curve profile is irregular compared to the slowest velocities. The coordination number depends also on the spreading speed since a 50 mm/s spreading permits to obtain the best average coordination number (around 6). Finally, the

average grains size slightly increase according to the position in the powder bed for the highest speeds. It could be the segregation phenomenon as smallest particles are mainly at the beginning of the plate. This study also shows that density evolves like coordination number in this case unlike with adhesion study. Coordination number can be considered as local density.

## 4 Discussions

The parametric study of material and process parameters permitted to show that some parameters have a significant impact on powder bed properties whereas some parameters seem not to have a major influence. First, surface roughness has a significant impact on powder flow and final powder bed properties. It is then an important parameter to consider when simulating powder spreading. Concerning the friction coefficient, it seems not to have an influence on the powder bed properties. On the other hand, adhesion parameter is very impacting the powder bed properties. Low adhesion

results in a homogeneous and dense powder bed. Whereas high adhesion produces an heterogeneous powder bed with clusters and cavities. Even if material parameters cannot be directly modified for a given powder sample, humidity affects directly adhesion energy so dry environment are preferable for the powder. It seems to have a threshold effect as adhesion energy is  $1 \text{ mJ/m}^2$  reasonable but it is preferable not to be more adhesive than that. According to these results, only adhesion must be identified precisely for a given powder sample and must be controlled in real process. Spreader speed is an important process parameter and its effect on powder bed quality was expected. A lower speed produces

**Fig. 9** Friction coefficient

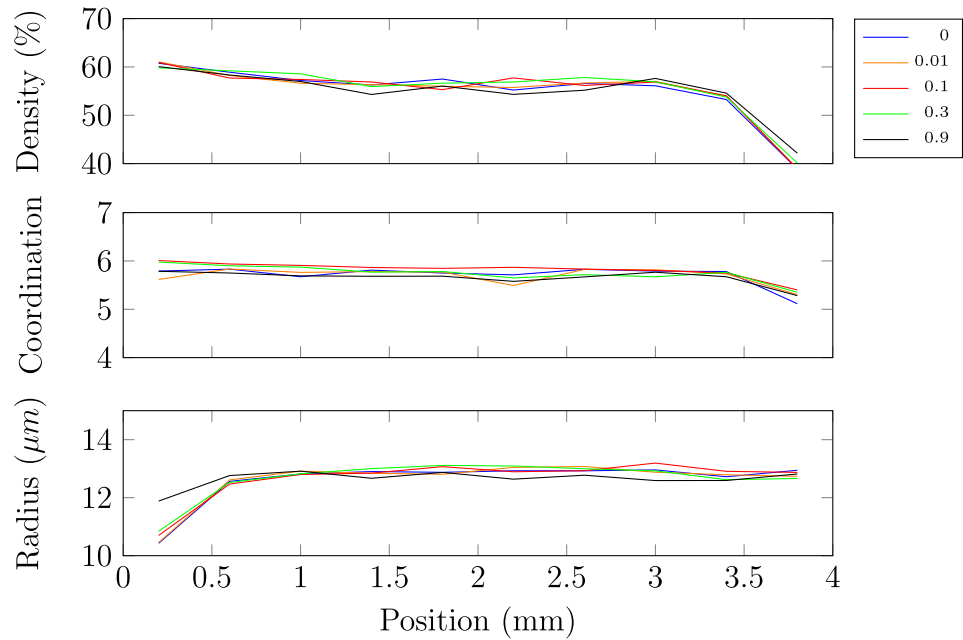


**Fig. 10** Adhesion energy

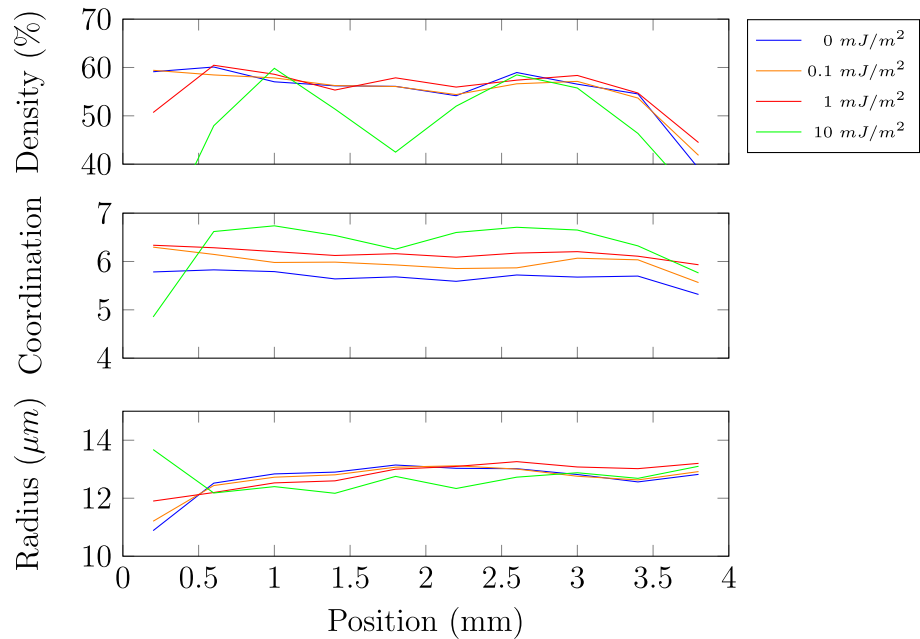


Fig. 11 Powder bed

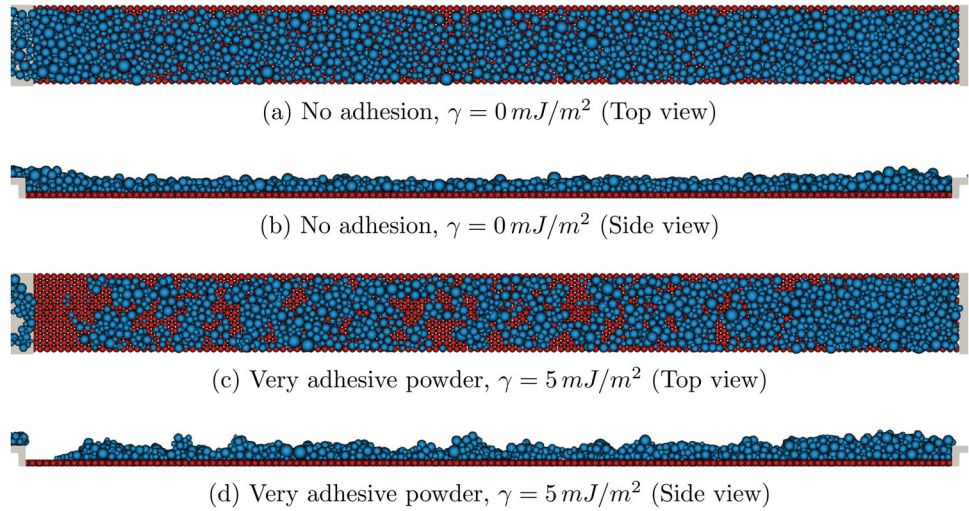
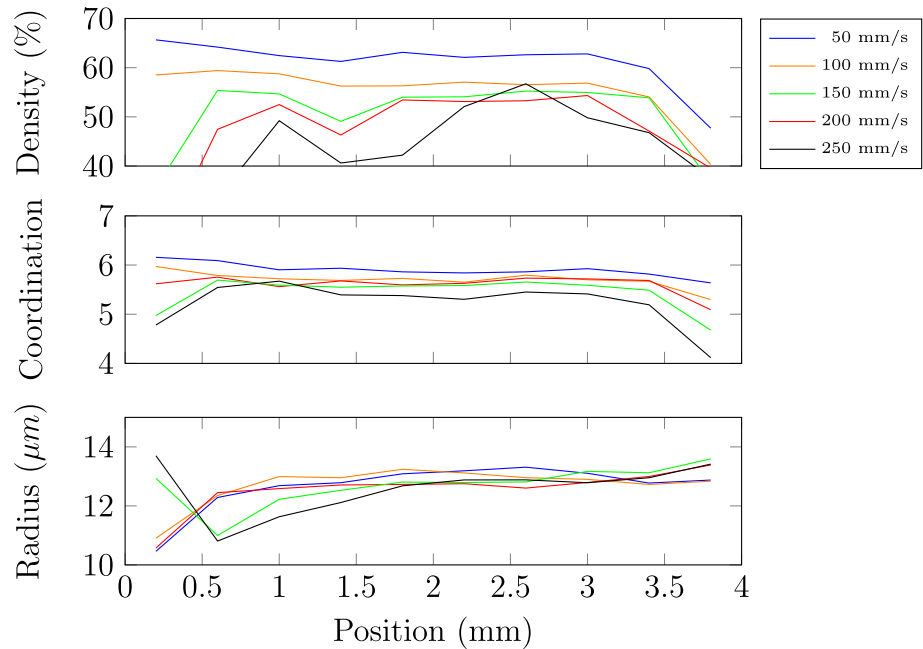


Fig. 12 Spreader speed



a better powder bed. Here, it also seems to have a threshold effect as for speeds above 100 mm/s, spreading generates heterogeneous powder bed. Finally, in the presented studies, the segregation phenomenon has not been clearly identified except a particular case when spreader speed is very high.

## 5 Conclusion

In order to produce the most representative simulations of real spreading, the material parameters of powder samples will have to be identified precisely. Since the adhesion energy is the only parameter to identify, the experimental testing of powder angle of repose can be realized in comparison

with equivalent simulations as shown by Meier et al. [8]. Except on the adhesion effect study, adhesion energy has been taken to 0 mJ/m<sup>2</sup> in order to eliminate the adhesion effect when studying effect of other parameters. However, it must be noted that powders always present at least a minimal amount of adhesion energy. More complete parametric studies will be computed in the future to investigate the effect of other process parameters and also the eventual coupling between several parameters. Finally, simulations with longer plates could be computed to try to identify segregation effect.

**Acknowledgements** This work is a part of Additive Factory Hub (AFH) platform. Simulations have been computed with GranOO workbench : [www.granoo.org](http://www.granoo.org).

## References

1. Zielinski J, Vervoort S, Mindt HW, Megahed M (2017) Influence of powder bed characteristics on material quality in additive manufacturing. *BHM Berg- und Hüttenmännische Monatshefte* 162:192–198
2. Haeri S (2017) Optimisation of blade type spreaders for powder bed preparation in additive manufacturing using dem simulations. *Powder Technol* 321:94–104
3. Fouda YM, Bayly AE (2019) A dem study of powder spreading in additive layer manufacturing. *Granul Matter* 22
4. Chen H, Chen Y, Liu Y, Wei Q, Shi Y, Yan W (2020) Packing quality of powder layer during counter-rolling-type powder spreading process in additive manufacturing. *Int J Mach Tools Manuf* 153:103553. <https://doi.org/10.1016/j.ijmachtools.2020.103553>
5. Chen H, Wei Q, Wen S, Li Z, Shi Y (2017) Flow behavior of powder particles in layering process of selective laser melting : numerical modeling and experimental verification based on discrete element method. *Int J Mach Tools Manuf* 123:146–159
6. Chen H, Wei Q, Zhang Y, Chen F, Shi Y, Yan W (2019) Powder-spreading mechanisms in powder-bed-based additive manufacturing: experiments and computational modeling. *Acta Mater* 179:158–171
7. Meier C, Weissbach R, Weinberg J, Wall WA, Hart AJ (2019) Critical influences of particle size and adhesion on the powder layer uniformity in metal additive manufacturing. *J Mater Process Technol* 266:484–501
8. Meier C, Weissbach R, Weinberg J, Wall WA, Hart AJ (2019) Modeling and characterization of cohesion in fine metal powders with a focus on additive manufacturing process simulations. *Powder Technol* 343:855–866
9. Parteli EJR, Pöschel T (2016) Particle-base simulation of powder application in additive manufacturing. *Powder Technol* 288:96–102
10. Haeri S, Wang Y, Ghita O, Sun J (2016) Discrete element simulation and experimental study of powder spreading process in additive manufacturing. *Powder Technol* 306:45–54
11. Hoeges S, Zwiren A, Schade C (2017) Additive manufacturing using water atomized steel powders. *Met Powder Rep* 72:111–117
12. Nan W, Pasha M, Bonakdar T, Lopez A, Zafar U, Nadimi S, Ghadiri M (2018) Jamming during particle spreading in additive manufacturing. *Powder Technol* 338:253–262
13. Cundall PA, Strack ODL (1979) A discrete numerical model for granular assemblies. *Géotechnique* 29:47–65
14. André D, Charles JL, Iordanoff I, Néauport J (2014) The granoo workbench, a new tool for developing discrete element simulations and its application to tribological problems. *Adva Eng Softw* 74:40–48
15. Hertz H (1882) Ueber die berührung fester elastischer körper. *J für die reine und angew Math* 92:156–171
16. Chen H, Xiao YG, Liu Y, Shi Y (2017) Effect of young's modulus on dem results regarding transverse mixing of particles within a rotating drum. *Powder Technol* 318:507–517
17. Johnson KL, Kendall K, Roberts AD (1971) Surface energy and the contact of elastic solids. *Proc R Soc* 324:301–313
18. Derjaguin BV, Muller VM, Toporov YP (1975) Effect of contact deformations on the adhesion of particles. *J Colloid Interface Sci* 53(2):314–326
19. Fouda, Yahia & Bayly, Andrew. (2019). A DEM study of powder spreading in additive layer manufacturing. *Granular Matter*. 22
20. Gladkyy A, Schwarze R (2014) Comparison of different capillary bridge models for application in the discrete element method. *Granul Matter* 16:911–920
21. Tan JH, Wong WLE, Dalgarno KW (2017) An overview of powder granulometry on feedstock and part performance in the selective laser melting process. *Addit Manuf* 18:228–255
22. Moreau JJ, Panagiotopoulos PD (1988) *Non-smooth mechanics and applications*. Springer, Berlin
23. André D (2012) *Modélisation par éléments discrets des phases d'ébauchage et de doucissage de la silice*, Ph.D. thesis, Université de Bordeaux
24. Coutias A, Romero L The quaternions with an application to rigid body dynamics. Technical Report, University of New Mexico, Albuquerque
25. Nguyen QB, Nai MLS, Zhu Z, Sun CN, Wei J, Zhou W (2017) Characteristics of inconel powders for powder-bed additive manufacturing. *Engineering* 3:695–700
26. Poiron P, Sommier N, Faugère AM, Evesque P (2004) Dynamics of size segregation and mixing of granular materials in a 3d-blender by nmr imaging investigation. *Powder Technol* 141:55–69